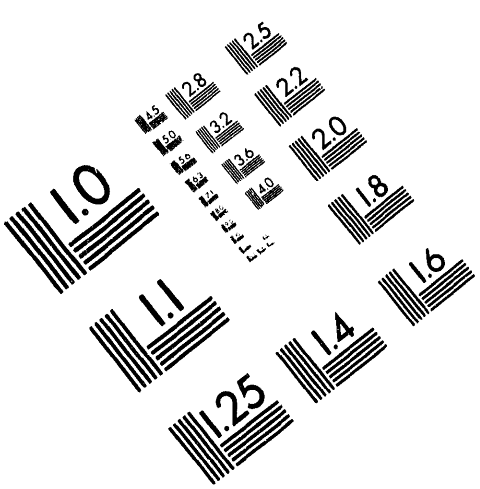

AIIM

Association for Information and Image Management
1100 Wayne Avenue, Suite 1100
Silver Spring, Maryland 20910
301/587-8202

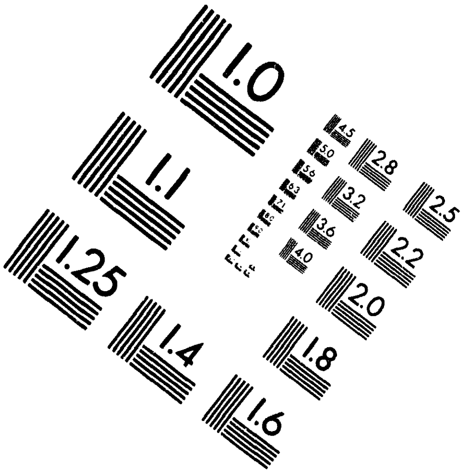

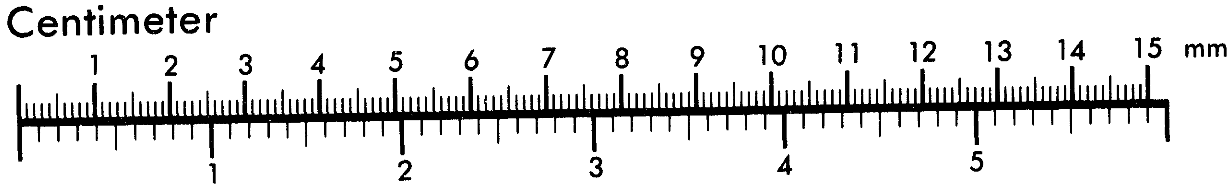

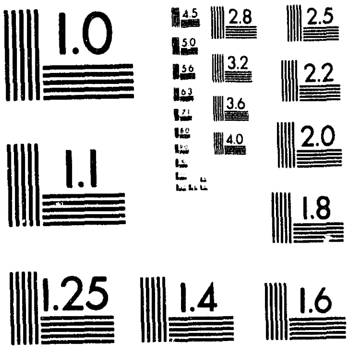

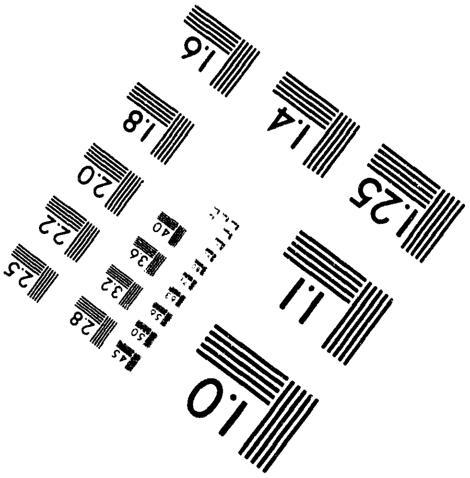

MANUFACTURED TO AIIM STANDARDS
BY APPLIED IMAGE, INC.

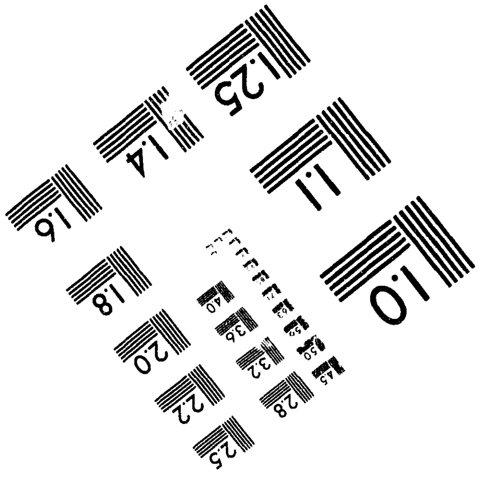

1 of 1

A GRADIENT METHOD FOR ANOMALOUS SMALL-ANGLE X-RAY SCATTERING

Pete R. Jemian
Materials Science Division
Argonne National Laboratory
Argonne, IL 60439

Julia R. Weertman
Northwestern University
Evanston, IL 60208

and

Gabrielle G. Long
National Institute of Standards and Technology
Gaithersburg, MD 20899

The submitted manuscript has been authored by a contractor of the U.S. Government under contract No. W-31-109-ENG-38. Accordingly, the U.S. Government retains a nonexclusive, royalty-free license to publish or reproduce the published form of this contribution, or allow others to do so, for U.S. Government purposes.

15 September 1992

DISCLAIMER

This report was prepared as an account of work sponsored by an agency of the United States Government. Neither the United States Government nor any agency thereof, nor any of their employees, makes any warranty, express or implied, or assumes any legal liability or responsibility for the accuracy, completeness, or usefulness of any information, apparatus, product, or process disclosed, or represents that its use would not infringe privately owned rights. Reference herein to any specific commercial product, process, or service by trade name, trademark, manufacturer, or otherwise does not necessarily constitute or imply its endorsement, recommendation, or favoring by the United States Government or any agency thereof. The views and opinions of authors expressed herein do not necessarily state or reflect those of the United States Government or any agency thereof.

/sm

Distribution:

1-2. M. J. Masek
3. B. D. Dunlap
4. M. B. Brodsky
5. J. D. Jorgensen
6. B. S. Brown
7. Editorial Office
8. Authors

This work is supported by the U.S. Department of Energy, Basic Energy Sciences, Materials Sciences, under contract No. W-31-109-ENG-38.

MASTER

DISTRIBUTION OF THIS DOCUMENT IS UNLIMITED

A GRADIENT METHOD FOR ANOMALOUS SMALL-ANGLE X-RAY SCATTERING

Pete. R. Jemian
Materials Science Division
Argonne National Laboratory
Argonne, IL 60439

Julia R. Weertman[1], and Gabriell G. Long[2]

15 September 1992

/sm

Work from Thesis

This work is supported by the U.S. Department of Energy, Basic Energy Sciences, Materials Sciences, under contract No. W-31-109-ENG-38.

[1] Dept. of Materials Science and Engineering, McCormick School of Engineering and Applied Science,Northwestern University, Evanston, IL 60208

[2] Ceramics Division, NITS, Gaithersburg, MD 20899

A Gradient Method for Anomalous Small-Angle X-ray Scattering

Pete R. Jemian[1], Julia R. Weertman
Department of Materials Science and Engineering, McCormick School of Engineering and Applied Science, Northwestern University, Evanston, IL 60208

and Gabrielle G. Long
Ceramics Division, National Institute of Standards and Technology, Gaithersburg, MD 20899

15 September 1992

Abstract

A new method of general applicability for analyzing data from anomalous dispersion small-angle X-ray scattering (ASAXS) measurements is described. ASAXS is used as a contrast variation method to label the scattering from a single element in a complex material containing several types of scatterers. The contrast variation is achieved through the anomalous dispersion of X-rays. Thus only one sample is required for a complete analysis. To label a scatterer by ASAXS, the atomic scattering factor of an element in the sample is varied by the selection of photon energies near the absorption edge of the element. Careful selection of the photon energies allows the contrast of only the labeled scatterer to change. Data from several small-angle scattering measurements, each conducted at a fixed energy, are combined in a single analysis. The gradient method, used as an extension to a standard SAXS data analysis method, is demonstrated by isolating the volume fraction size distribution of $Cr_{23}C_6$ in 9Cr-1MoVNb steel.

---

[1] present address: Materials Science Division, Argonne National Laboratory, Argonne, IL 60439

printed: 15 September 1992

A Gradient Method for Anomalous Small-Angle X-ray Scattering

Pete R. Jemian,[a] Julia R. Weertman

Department of Materials Science and Engineering,
McCormick School of Engineering and Applied Science,
Northwestern University, Evanston, IL 60208

and Gabrielle G. Long

Ceramics Division,
National Institute of Standards and Technology,
Gaithersburg, MD 20899

A new method of general applicability for analyzing data from anomalous dispersion small-angle X-ray scattering (ASAXS) measurements is described. ASAXS is used as a contrast variation method to label the scattering from a single element in a complex material containing several types of scatterers. The contrast variation is achieved through the anomalous dispersion of X-rays. Thus only one sample is required for a complete analysis. To label a scatterer by ASAXS, the atomic scattering factor of an element in the sample is varied by the selection of photon energies near the absorption edge of the element. Careful selection of the photon energies allows

---

[a] *present address:* Materials Science Division, Argonne National Laboratory, Argonne, IL 60439

the contrast of only the labeled scatterer to change. Data from several small-angle scattering measurements, each conducted at a fixed energy, are combined in a single analysis. The gradient method, used as an extension to a standard SAXS data analysis method, is demonstrated by isolating the volume fraction size distribution of $Cr_{23}C_6$ in 9Cr-1MoVNb steel.

I. INTRODUCTION

Small-angle X-ray scattering (SAXS) has become well-recognized as a premier technique for the characterization of a wide variety of materials. (Guinier & Fournet, 1955, Brumberger, 1965, Kostorz, 1979, Glatter & Kratky, 1982) SAXS can be used to obtain microstructural parameters such as the mean size, total interfacial surface area per unit volume, volume fraction, and size distribution of scatterers with characteristic linear dimensions on the scale of nanometers to micrometers. Precipitates, voids, oxides, and composition-modulated structures are typical of the scatterers observed in condensed matter samples. Microstructural parameters are extracted from the magnitude and shape of the X-ray intensity profile scattered at small angles from the transmitted beam. Ordinarily, SAXS does not discriminate with respect to the scattering species. For materials containing several scattering species, the measured scattering pattern represents a combination of the individual patterns from each of the various scattering types present. The size distribution of a particular species can be calculated from the whole for the special case in which its scattering is well-separated from all the rest. This situation arises when the size range of the given species is very different from that of the other scatterers. However, in general, it is impossible to separate the scattering of one species from the total (measured) pattern.

In neutron scattering, one experimental technique commonly used to separate scattering species is contrast variation. In Isotopic substitution Small-Angle Neutron Scattering (Simon, Lyon, & de Fontaine, 1985) (ISANS), the contrast of one scatterer is varied while the contrasts of all the other scatterers are kept constant. An example is the substitution of deuterium for hydrogen. Similar to isomorphous replacement, ISANS requires a different sample for each variation in contrast. For complicated materials, this means that many sample preparations and many independent SANS measurements are required. An inherent problem with this technique is the necessity for insuring that, except for the isotopic substitutions, the samples are identical.

For X-rays, contrast variation is available by changing the energy of the incident photons, thereby making use of anomalous dispersion. We will call this technique Anomalous dispersion Small-Angle X-ray Scattering (ASAXS). The same sample is used for all measurements, avoiding the potential microstructural differences among samples associated with ISANS. With the current generation of high-intensity, broad spectrum, synchrotron radiation X-ray sources, ASAXS is available for the study of scatterers containing *3d* transition elements and the lanthanides, which are fundamental to many important complex materials.

ASAXS techniques are based on the fact that the atomic scattering factor of a particular element changes significantly when the energy of the incident photons approaches the binding energy of one of the core electrons of that element. Thus the ASAXS contrast variation is a continuous function of photon energy, allowing the selection of numerous contrasts for each sample. Shevchik (Shevchik, 1977) presented a method for frequency-modulated X-ray diffraction using anomalous dispersion. Shevchik's method relies on the continuous nature of the scattering contrast as a function of photon energy to extract information about the labeled atom. A theory of *differential* anomalous scattering has been presented elsewhere (Fuoss, Eisenberger, Warburton, & Bienenstock, 1981). With the differential technique, two experiments, each at a different photon energy, are combined in a single analysis. The differential technique is suitable for both ASAXS and ISANS. In the present paper, we describe a *gradient* method for collecting and analyzing the data from an ASAXS experiment. With the gradient method, an arbitrary number of measurements, each at a different photon energy, are combined together in a single analysis in a manner similar to that proposed by Shevchik.

II. THEORY

A. SAXS

Assume that a sample consists of a matrix that contains scatterers of uniform composition and shape, randomly-dispersed, and distributed in size, and that scattering interference between the scatterers is negligible. The differential scattering cross-section of the small-angle scattering from such a sample, $d\Sigma/d\Omega(h)$, can be written as:

$$\frac{d\Sigma}{d\Omega}(h) = |\Delta\rho|^2 \int_0^\infty G(h,r)\,\varphi(r)\,dr, \tag{1}$$

where $h = (4\pi/\lambda)\sin(\theta)$, λ is the wavelength of the incident photons, 2θ is the scattering angle, $|\Delta\rho|^2$ is the scattering contrast of a scatterer with respect to the matrix, $G(h,r)$ describes the morphology and volume of the scatterers and instrumental effects such as collimation and the incident spectrum, and $\varphi(r)dr$ is the volume fraction of scatterers of characteristic linear dimension r in a bin of width dr. The X-ray scattering contrast,

$$|\Delta\rho|^2 \equiv |\rho_s - \rho_0|^2 = \left| r_e \sum_Z \Delta c_Z\, f_Z \right|^2, \tag{2}$$

is the square of the difference in scattering length density between the scatterer (ρ_s) and the matrix (ρ_0). Here $r_e = 2.818$ fm and Z is the atomic number of the element with concentration difference Δc_Z between the scatterers and the matrix. Taking r as the sphere radius, the morphology term for spherical scatterers, assuming perfect collimation and monochromatic incident radiation,

$$G(h,r) = \frac{4\pi}{3} r^3 \left| \frac{3}{(hr)^3}[\sin(hr) - (hr)\cos(hr)] \right|^2. \tag{3}$$

B. Anomalous Dispersion

For X-ray scattering at small angles, the atomic scattering factor of element Z,

$$f_Z(E) = Z + f'_Z(E) + i f''_Z(E), \tag{4}$$

where the latter two terms are the corrections due to anomalous dispersion. When the energy, E, of the incident photons, is near the binding energy, E_b, of one of the core electrons in element Z, the real part of the anomalous dispersion corrections,

$$f'_Z(E) \simeq g_b \ln \left| \frac{E_b - E}{E_b} \right|, \tag{5}$$

where g_b is the oscillator strength (James, 1965) of the core electron. The imaginary part, f'', is due to absorption in the sample. For E slightly below E_b, f'' is small and independent of E. When E becomes greater than E_b, there is a significant increase in the absorption of X-rays, as required for the liberation of the bound electron. Anomalous dispersion effects continue to be important even for energies far removed from the vicinity of absorption edges. Thus it is necessary to include the f' and f'' terms for all elements in the system to be studied.

The core electron binding energies vary in a systematic fashion with atomic number, as shown in Fig. 1. The core electron binding energies of the K shell electrons are well separated to allow their use in labeling the scattering due to individual elements. For example, Fig. 2a, based on the calculations of Cromer and Liberman (Cromer & Liberman, 1970) demonstrates this separation for two elements (V and Cr) with adjacent atomic numbers ($Z = 23$ and 24) at energies near the K absorption edge.

The core electron binding energies of the L shell electrons have a more complicated separation, as shown in Fig 2b for the elements La and Ce (atomic numbers 57 and 58). There are three edges for the L electrons. ASAXS measurements are conducted below the L_{III} edge to avoid fluorescence (to be discussed later).

C. ASAXS

The energy-dependent scattering contrast,

$$|\Delta\rho|^2(E) = \left| r_e \sum_Z \Delta c_Z \left[Z + f'_Z(E) + i f''_Z(E) \right] \right|^2 . \tag{6}$$

As already noted for samples of complex materials with more than one type of scatterer, it is not possible to solve Eq. (1) for the size distribution of each scatterer by means of a single photon energy experiment. The small-angle scattering from a complex material,

$$\frac{d\Sigma}{d\Omega}(h,E) = \sum_s |\Delta\rho|_s^2(E) \int_0^\infty G_s(h,r)\,\varphi_s(r)\,dr, \tag{7}$$

where the sum is over all the different species s of scatterers. However it is possible to obtain a weighted size distribution from the measured intensity. We call that weighted size distribution the ***scattering strength distribution***, defined as:

$$x_T(r,E) \equiv \sum_s |\Delta\rho|_s^2(E)\,\varphi_s(r), \tag{8}$$

where the sum is over all the different types of scatterer. The scattering strength distribution for each different photon energy is obtained as the solution of

$$\frac{d\Sigma}{d\Omega}(h,E) = \int_0^\infty G(h,r)\,x_T(r,E)\,dr, \tag{9}$$

assuming that all the scatterers can be described by a common morphology term $G(h,r)$. Solution of Eq. (8) for the individual $\varphi_s(r)$ is then contingent upon obtaining sufficient variation in $|\Delta\rho|_s^2(E)$ from experiments at different photon energies to label each scatterer.

III. EXPERIMENTAL

A. Photon Energy Selection

The energy spread of the incident X-rays affects the selection of the photon energy for anomalous scattering experiments. For a double crystal monochromator at an X-ray synchrotron, the intensity in the tail of the energy spectrum is proportional to $(E_0 - E)^{-4}$ where E_0 is the incident photon energy. Fluorescence occurs for $E > E_b$, where E_b is the absorption edge to be used in the anomalous scattering experiment. E_0 should be chosen to minimize the fluorescence, since it increases the background. Because of fluorescence, anomalous scattering measurements are conducted with $E_0 < E_b$.

Another consideration when $E_0 < E_b$ is the intensity of resonant Raman scattering (RRS), another form of inelastic scattering. The intensity of RRS (Sparks, 1974, Eisenberger, Platzman, & Winick, 1976) goes as $\sim 1/(E_b - E_0)$. The success of an ASAXS experiment depends on producing a large change in $f_Z(E_0)$ as the photon energy moves away from the absorption edge of element Z. The maximum change in $f'_Z(E_0)$ occurs at $E_0 = E_b$, as seen from Eq. (5). However, the presence of RRS and the long energy tail of the monochromator spectrum require that the photon energy nearest the absorption edge be chosen at least 2 to 3 monochromator resolution elements below E_b.

The photon energy farthest from the absorption edge is chosen to obtain the maximum difference in $f'(E_0)$ from the near-edge value while holding nearly constant the scattering factors of all other elements in the system. For the Cr K absorption edge, $E_b = 5989$ eV. The difference between the near and far energies can be about 200 eV, which gives $\Delta f \sim 3$ e.u., or $\Delta f/f \sim 0.1$ at $h = 0$ (Fig. 3).

B. Gradient Method

The gradient method for ASAXS is useful when one can find a range of photon energies such that the scattering contrast of only the labeled scatterer changes while that of the other scatterers remains constant. In this case, from Eq. (8),

$$\left.\frac{\partial x_T}{\partial|\Delta\rho|_1^2}\right|_{r,|\Delta\rho|_2^2,|\Delta\rho|_3^2,\ldots} = \varphi_1(r). \tag{10}$$

An example of a complex system to which the gradient method is applicable is the ferritic/martensitic steel 9Cr-1MoVNbwhich has small additions of the strong carbide formers V and Nb. The nominal composition of this alloy is given in Table I. Complete details of the ASAXS experiment are given elsewhere (Jemian, Weertman, Long, & Spal, 1991). Three precipitates have been observed by transmission electron microscopy (Maziasz & Klueh, 1990, Maziasz & Klueh, 1991): NbC, VC, and $Cr_{23}C_6$. The total amount of extracted precipitate observed by TEM was a few weight percent. Broad beam X-ray energy dispersive spectroscopy (Maziasz & Klueh, 1991) (XEDS) showed the partition of extracted precipitates to be 10-15% VC+NbC and 85-90% $Cr_{23}C_6$. From the alloy composition, if all of the V and Nb atoms are in the carbides, one would expect about four or five times more VC than NbC.

The binding energy of Nb K electrons, 18986 eV, is at the upper limit of the monochromator at many synchrotron X-ray beam lines. The binding energies of V and Cr K electrons, 5465 and 5989 eV, respectively, are near the low end of the energy range accessible to the hard X-ray monochromator. Thus, the K edges of V, Cr, and Nb are all accessible. However, the low observed amount of NbC implies that its scattered intensity would be quite low. The large expected volume fraction of $Cr_{23}C_6$ scatterers, combined with a significant Δc_{Cr} makes the K edge of Cr the most suitable for a demonstration of the ASAXS gradient method. ASAXS experiments at the Cr K edge were made to label the scattering from a distribution of $Cr_{23}C_6$ in the 9Cr-1MoVNb steel.

Anomalous dispersion corrections, $f'(E)$ and $f''(E)$ for Cr, were calculated from EXAFS-type transmission measurements (Jemian, Weertman, Long, & Spal, 1991) from a sample of the 9Cr-1MoVNb steel. These are compared in Fig. 3 with theoretical calculations (Cromer & Liberman, 1970). Agreement to within ±0.2 electron units was found between the experimental and theoretical values (disregarding the EXAFS structure observed on the high-energy side of the absorption edge). Also indicated in Fig. 3 are the three photon energies (a, b, and c) used for the ASAXS measurements.

The calculated scattering contrasts of NbC, VC, and $Cr_{23}C_6$ are plotted in Fig. 4 for the three energies we used near the Cr K edge. Across this energy range, the contrast of NbC is nearly constant and quite low. While the scattering contrast of VC is two to three times greater than that of $Cr_{23}C_6$, the scattered intensity from the $Cr_{23}C_6$ precipitates in the 9Cr-1MoVNb steel should be greater because of their larger volume fraction and larger size (as known from TEM measurements, Maziasz & Klueh, 1991). Also, the change in the scattering contrast of VC across this energy range is small while the contrast of $Cr_{23}C_6$ changes by a factor of three. The change in the scattering contrast of $Cr_{23}C_6$ is due to the decrease in the atomic scattering factor of Cr produced by anomalous dispersion. While there is also Cr in the matrix, its concentration in the $Cr_{23}C_6$ particles is much higher.

The ASAXS intensity curves at the three energies near the Cr K edge are shown in Fig. 5 for the sample aged 5000 h at 755 K. The data points correspond to the normalized measured intensities. A scattering strength size distribution, $x_T(r, E)$, was calculated from each curve, after Eq. (9), using a maximum entropy constraint (Potton, Daniell, & Rainford, 1986). In the calculations, it is assumed that the carbides are spherical, as described in Eq. (3). The three distributions are shown in Fig. 6. The lines shown in Fig. 5 are the intensities back-calculated from $x_T(r, E)$. The solid lines in Fig. 6 have been drawn to guide the eye.

The slope of a plot of $x_T(r, E)$ *vs.* $|\Delta\rho|^2_{\mathrm{Cr_{23}C_6}}(E)$,

$$\left.\frac{\partial x_T(r, E)}{\partial |\Delta\rho|^2_{\mathrm{Cr_{23}C_6}}(E)}\right|_{r, |\Delta\rho|^2_{NbC}, |\Delta\rho|^2_{VC}, \dots} \simeq \varphi_{\mathrm{Cr_{23}C_6}}(r), \tag{11}$$

gives the volume fraction size distribution of chromium carbide, $\varphi_{\mathrm{Cr_{23}C_6}}(r)$, as shown in Fig. 7. The form of Eq. (11) reflects the fact that $|\Delta\rho|^2_{\mathrm{VC}}$ and $|\Delta\rho|^2_{\mathrm{NbC}}$ change negligibly over the 200 eV energy range of the scattering experiments near the Cr K absorption edge. Fig. 8 shows $\varphi_{\mathrm{Cr_{23}C_6}}(r)$ obtained for the 9Cr-1MoVNb steel sample subjected to 5000 h aging at 755 K. The symbols indicate the values derived from Eq. (11). The vertical bars are the standard deviation of each value and indicate the estimated margin of error in the analysis. These errors represent the level of confidence one can expect from the size distribution. With such low signal-to-noise ratios, the small features in the size distribution were taken to be statistically insignificant. The curve was then smoothed (solid lines) to guide the eye. The estimated total volume fraction of $\mathrm{Cr_{23}C_6}$ is 0.0071(1). The volume-weighted mean diameter is 194(1) nm and the half-width of the distribution is 134(2) nm.

C. Discussion

Anomalous scattering measurements can be used to label a single type of scatterer in a complex system using a single sample. Through the use of a gradient method involving three or more experiments, a statistical analysis is possible which provides an estimate of the systematic error in the procedure.

The gradient method may be applied either to the scattering strength distributions, as in Eq. (10) or to the differential scattering cross-sections themselves before data reduction, as in

$$\left.\frac{\partial \frac{\mathrm{d}\Sigma}{\mathrm{d}\Omega}(h, E)}{\partial |\Delta\rho|^2_1(E)}\right|_{h, |\Delta\rho|^2_2, |\Delta\rho|^2_3, \dots} = \int_0^\infty G_1(h, r)\, \varphi_1(r)\, \mathrm{d}r. \tag{12}$$

Thus the gradient method may be incorporated into standard methods of small-angle scattering analysis. In the example presented here, the gradient method has been used to extract the particle size distribution of $Cr_{23}C_6$ precipitates from an overall distribution weighted by the additional effects of distributions of VC and NbC precipitates.

We mention in passing that the gradient method may be extended to small-angle neutron scattering from bulk ferromagnetic polycrystalline samples containing paramagnetic scatterers. For magnetic SANS, the scattering contrast is a continuous function of the angle between the scattering vector and a saturation magnetic field applied to the sample. Compare this with ASAXS in which the scattering contrast is a continuous function of photon energy.

Application of the gradient method is usually limited in several respects. Fundamentally, the scattering contrasts of all the unlabeled scatterers must be held constant (or nearly so) for all experiments. This requirement is relaxed as the relative amount of unlabeled scatterers decreases. The scattering contrast is proportional to Δc_Z^2; only elements with a large difference in the atomic enrichment between the scatterer and the matrix can be labeled. A high-intensity, broad spectrum source of X-rays, such as synchrotron radiation, is required to obtain the contrast variation from a typical material where the volume fraction of labeled scatterers may be on the order of 1%.

At the National Synchrotron Light Source, the available range of photon energies, typically from 5 to 20 keV, allows one to probe the anomalous dispersion effects of the 3*d* transition elements and the lanthanides. On the low energy end of this range, absorption along the optical path is usually the limiting factor. The highest energy is limited by the available spectrum of the source. For double-crystal monochromators, the energy bandpass and long tails of the double-crystal monochromator spectrum limit how close to the absorption edge one can select photon energies without being affected by fluorescence. In turn, these limit the maximum change in $\Delta f/f$ possible. However, even in the case of very small $\Delta E/E$, lifetime broadening of the core hole (Shevchik, 1977) limits $\Delta f/f$ to ca. 30%.

IV. CONCLUSIONS

To use anomalous dispersion, the scatterer to be examined must contain an element with an absorption edge that is accessible to a synchrotron X-ray beam line monochromator. This generally includes the *3d* transition elements and the lanthanides. Additionally, a scatterer containing the labeled element must comprise a significant volume fraction of the sample. The concentration of the labeled element in the scatterer must differ significantly from that in the matrix. ASAXS has an advantage over ISANS in that only one sample is required for a complete X-ray analysis.

It has been shown that the anomalous dispersion effect is sufficiently localized in photon energy to allow the labeling of a single scattering species by contrast variation. Variation of the incident photon energy by ca. 200 eV near the binding energy of a K electron of a *3d* transition element is sufficient to obtain a change in $f'(E)$ of $2 \sim 3$ e.u. To illustrate the effect of this anomalous dispersion difference on the scattering contrast, a change of about a factor of three in the scattering contrast of $Cr_{23}C_6$ in a 9Cr-1MoVNb steel was calculated for a 200 eV energy variation near the Cr K absorption edge.

The gradient method relies upon the ability of the experimenter to vary the scattering contrast of the labeled scatterer while holding the contrasts of the other scatterers constant or nearly so. To illustrate, the gradient method was used to label the size distribution of a single scatterer ($Cr_{23}C_6$) in a complex system (9Cr-1MoVNb steel) and to assess its statistical reliability through the use of experimental data from several different scattering contrasts. X-ray anomalous dispersion was used as the contrast variation mechanism. Information from complementary techniques, such as TEM and XEDS, was useful in the analysis. Application of the gradient method was made by building upon existing data analysis techniques. A method for extending the gradient method to magnetic SANS has also been suggested.

ACKNOWLEDGMENTS

This research was supported in part by the United States Department of Energy under contract DE-FG-02-86ER45229 and in part by NIST which is supported by the United States Department of Commerce. This research was carried out at beam line X23A3 of the National Synchrotron Light Source, Brookhaven National Laboratory. The NSLS is supported by the United States Department of Energy, Division of Materials Sciences and Division of Chemical Sciences.

This work was performed under the auspices of the U. S. Department of Energy, Division of Materials Science, Office of Basic Energy Sciences under contract W-31-109-ENG-38.

REFERENCES

BRUMBERGER, H. (1965). *Small-Angle X-ray Scattering*, Syracuse University: Gordon and Breach.

CROMER, D.T. & LIBERMAN, D. (1970). *J. Chem. Phys.* **53**.5, 1891-1898.

EISENBERGER, P., PLATZMAN, P.M., & WINICK, H. (1976). *Phys. Rev. B* **13**.6, 2377-2380.

FUOSS, P.H., EISENBERGER, P., WARBURTON, W.K., & BIENENSTOCK, A. (1981). *Phys. Rev. Lett.* **46**, 1537-1540.

GLATTER, O. & KRATKY, O. (1982). *Small-Angle X-ray Scattering*, London: Academic Press.

GUINIER, A. & FOURNET, G. (1955). *Small-Angle Scattering of X-rays*, New York: John Wiley and Sons.

JAMES, R.W. (1965). *The Optical Principles of the Diffraction of X-rays*, volume II, Ithaca, NY: Cornell University Press.

JEMIAN, P.R., WEERTMAN, J.R., LONG, G.G., & SPAL, R.D. (1991). *Acta Metall. Mater.* **39**.11, 2477-2487.

KOSTORZ, G. (1979). "Small Angle Scattering and its Application to Material Science," in *Neutron Scattering*, edited by Kostorz, G., vol. 15, New York: Academic Press, pp. 227-289.

MAZIASZ, P.J. & KLUEH, R.L. (1990). *Effects of Radiation on Materials: 14th International Symposium* (edited by Stoller, R.E. & Kumar, A.S.), ASTM STP

1046, Vol. I, p. 35. Philadelphia, PA: American Society for Testing and Materials.

MAZIASZ, P.J. & KLUEH, R.L. (1991). *Effects of Radiation on Materials: 15th International Symposium* (in press). Philadelphia, PA: American Society for Testing and Materials.

POTTON, J.A., DANIELL, G.J., & RAINFORD, B.D. (1988). *J. Appl. Cryst.* **21**, 663-668.

SHEVCHIK, N.J. (1977). *Phil. Mag.* **35**, 805-809, 1289-1298.

SIMON, J.P., LYON, O., & DE FONTAINE, D. (1985). *J. Appl. Cryst* **18**, 230-236.

SPARKS, JR., C.J. (1974). *Phys. Rev. Lett.* **33**, 262-265.

FIGURES

FIG. 1. Core electron binding energies (absorption edges) accessible in the synchrotron X-ray region.

FIG. 2. Anomalous dispersion terms $f'(E)$ and $f''(E)$ *vs.* photon energy, calculated by the method of Cromer and Liberman (Cromer & Liberman, 1970). (a) For vanadium and chromium ($Z = 23$ and 24), and (b) for lanthanum and cerium ($Z = 57$ and 58). The three different L-electron binding energies are indicated for Ce.

FIG. 3. Chromium anomalous dispersion terms $f'(E)$ and $f''(E)$ *vs.* photon energy, near the Cr K edge (5989 eV). The symbols are experimental values calculated from transmission data of the 9Cr-1MoVNb steel, while the solid lines are calculated by the method of Cromer and Liberman (Cromer & Liberman, 1970). The energies used for the ASAXS measurements are indicated as $a = 5974$, $b = 5949$, and $c = 5789$ eV (Jemian, Weertman, Long, & Spal, 1991).

FIG. 4. Calculated scattering contrasts of NbC, VC, and $Cr_{23}C_6$ with respect to the matrix for three energies near the Cr K edge (5989 eV). Energies a, b, and c refer to the energies indicated in Fig. 3 (Jemian, Weertman, Long, & Spal, 1991).

FIG. 5. SAXS from a sample of 9Cr-1MoVNb steel aged 5000 h at 755 K. Size distributions (see Fig. 6) are calculated from the experimental data (symbols). From these

distributions, the intensity curves are back-calculated for comparison with the experimental data. Curves *a*, *b*, and *c* refer to the photon energies indicated in Fig. 3 (Jemian, Weertman, Long, & Spal, 1991).

FIG. 6. Scattering strength size distributions, $x_T(r, E)$, calculated from the experimental data of Fig. 5. Curves *a*, *b*, and *c* refer to the photon energies indicated in Fig. 3 (Jemian, Weertman, Long, & Spal, 1991).

FIG. 7. Illustration of the ASAXS gradient method for two diametral bins (86 and 250 nm) in the $Cr_{23}C_6$ volume fraction size distribution of the sample aged at 755 K (Jemian, Weertman, Long, & Spal, 1991).

FIG. 8. Volume fraction size distribution of $Cr_{23}C_6$ in 9Cr-1MoVNb steel, determined by the ASAXS gradient method. The sample was aged 5000 h at 755 K. The vertical bars represent the slope of the gradient analysis. The solid line is smoothed to guide the eye (Jemian, Weertman, Long, & Spal, 1991).

TABLES

TABLE I. Nominal composition (weight percent) of 9Cr-1MoVNb steel Carpenter Technology heat #30394. The principal alloying elements are Fe, C, Cr, Mo, V, and Nb.

C	N	Al	Si	P	Ti	V	Cr
.084	.053	.014	.4	.01	.005	.198	8.57
Mn	Fe	Co	Ni	Cu	Nb	Mo	W
.46	balance	.055	.09	.04	.073	1.02	.05

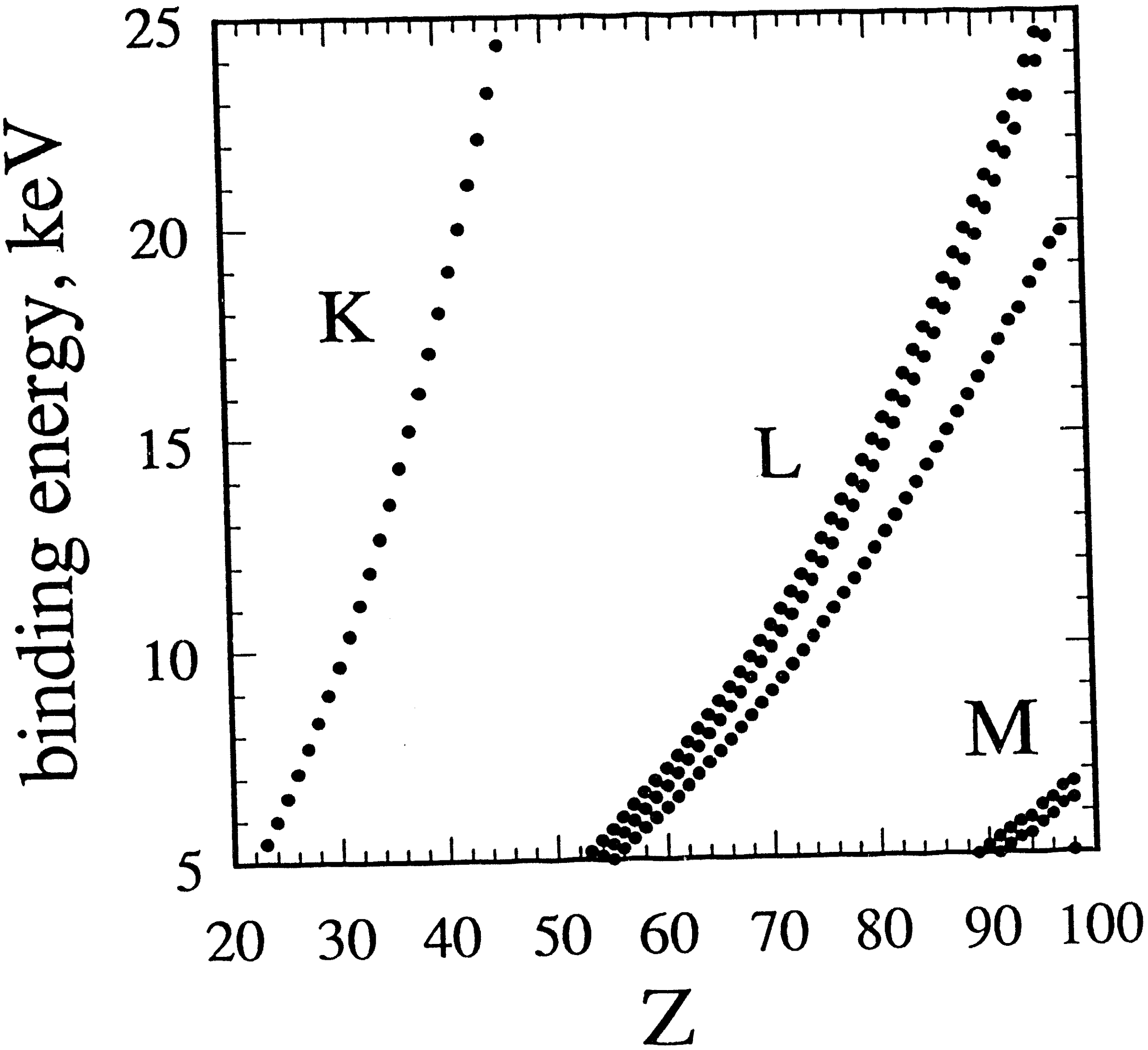
25
20
15
10
5
binding energy, keV
20
30
40
50
60
70
80
90
100
Z
K
L
M

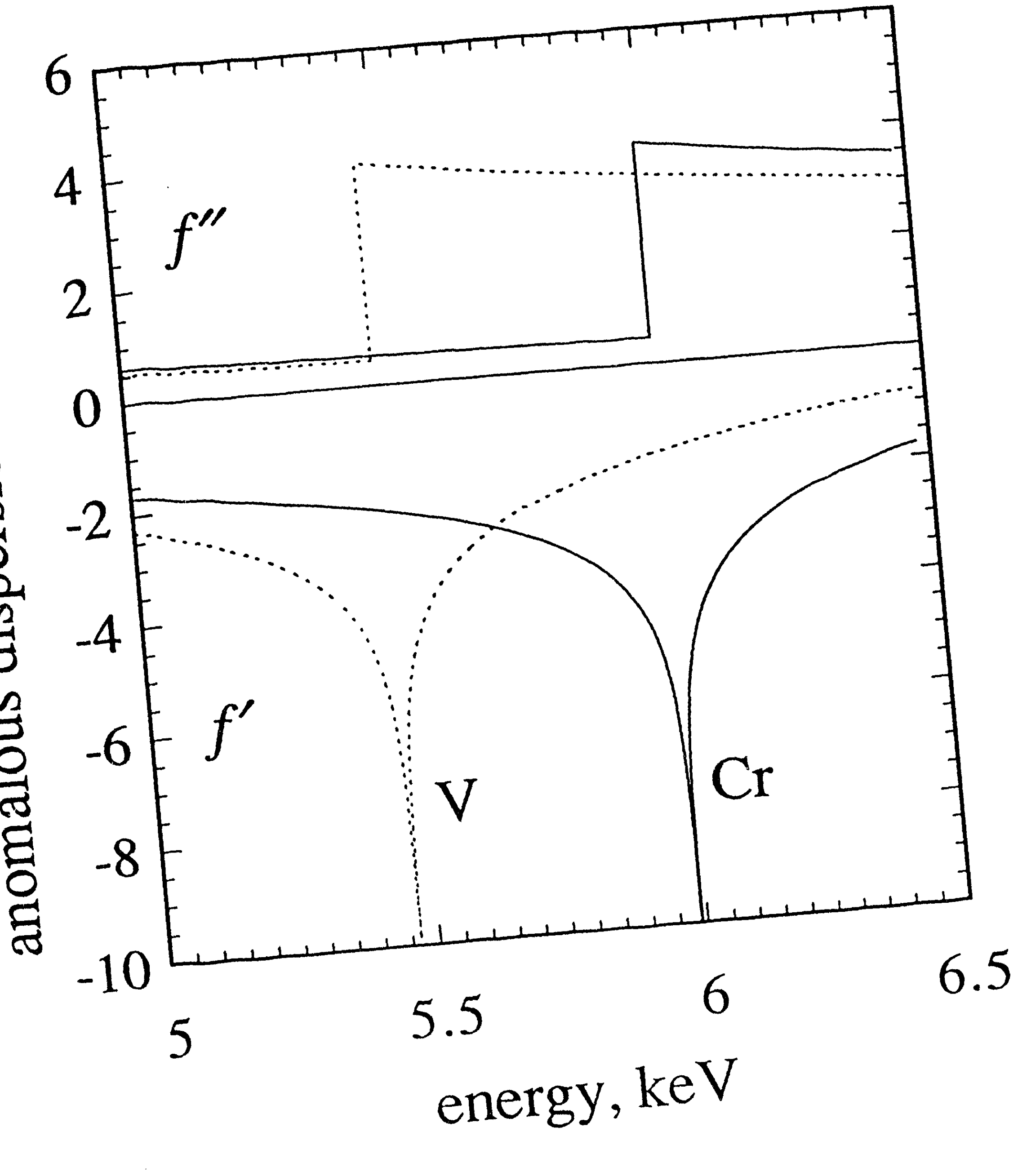
6
4
2
0
-2
-4
-6
-8
-10
anomalous dispersion terms, e.u.
f''
f'
V
Cr
5
5.5
6
6.5
energy, keV

2a

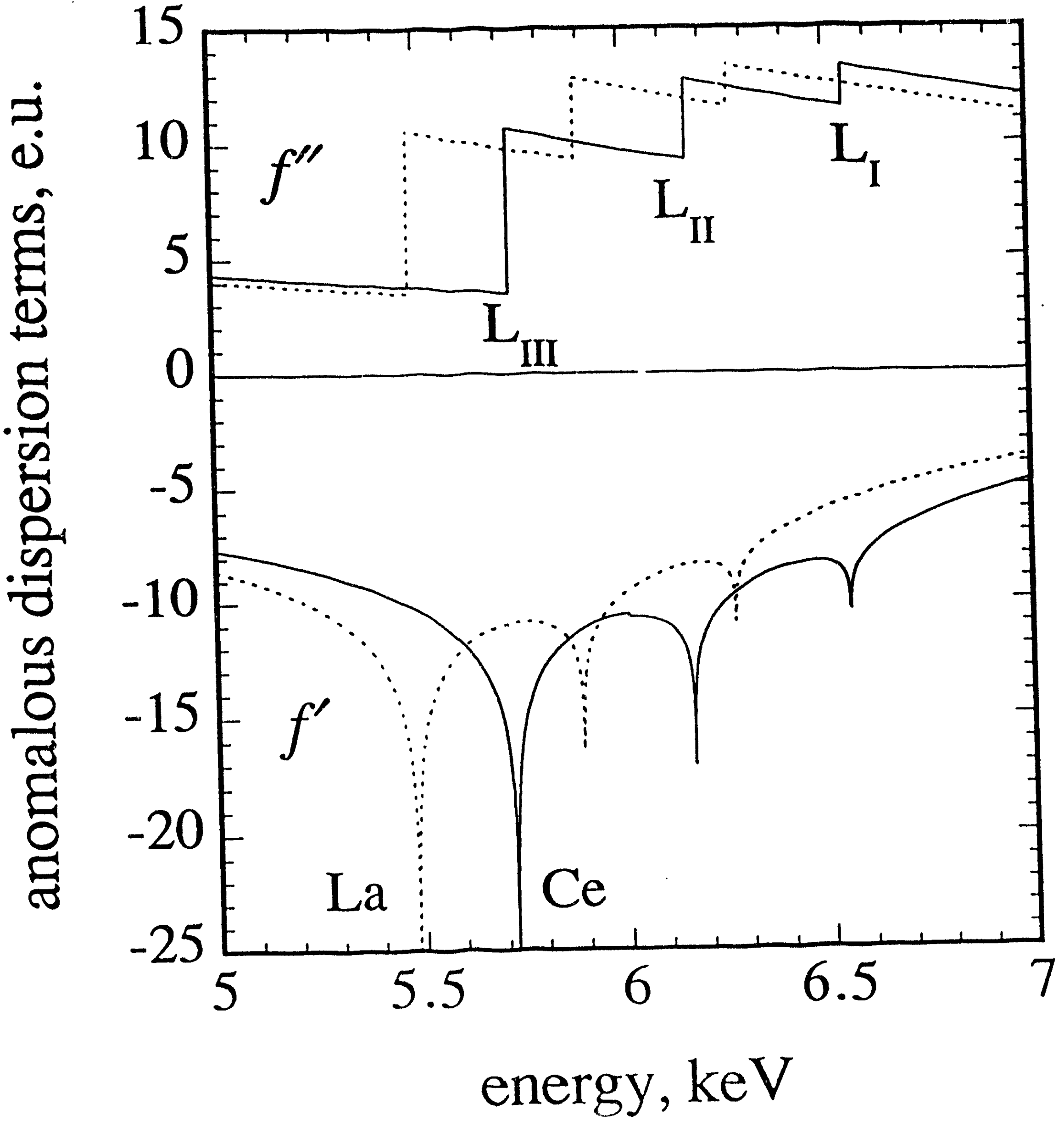
15
10
5
0
-5
-10
-15
-20
-25
anomalous dispersion terms, e.u.
f''
L_{III}
L_{II}
L_{I}
f'
La
Ce
5
5.5
6
6.5
7
energy, keV

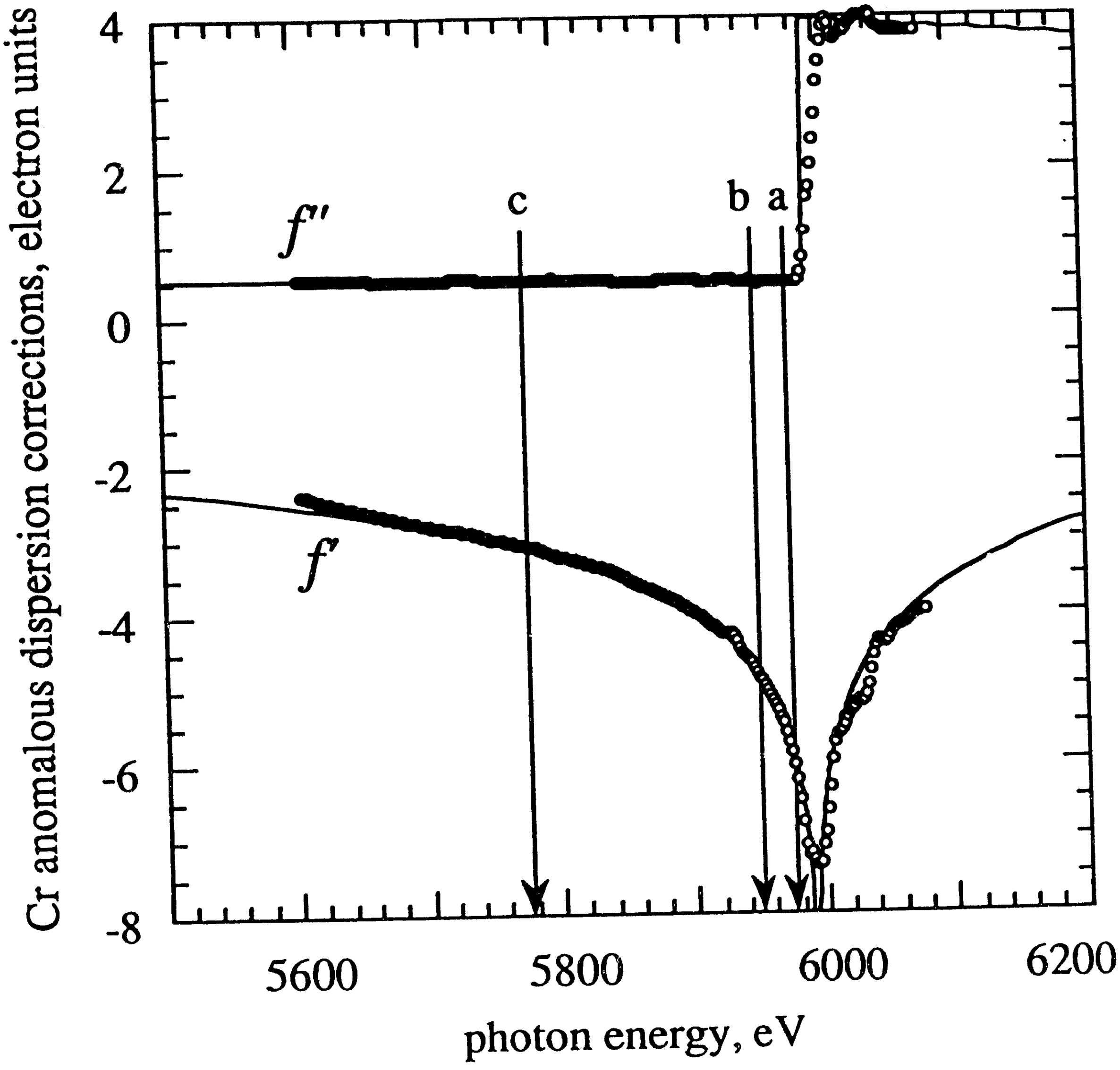

Cr anomalous dispersion corrections, electron units
4
2
0
-2
-4
-6
-8
5600
5800
6000
6200
photon energy, eV
f''
f'
c
b
a

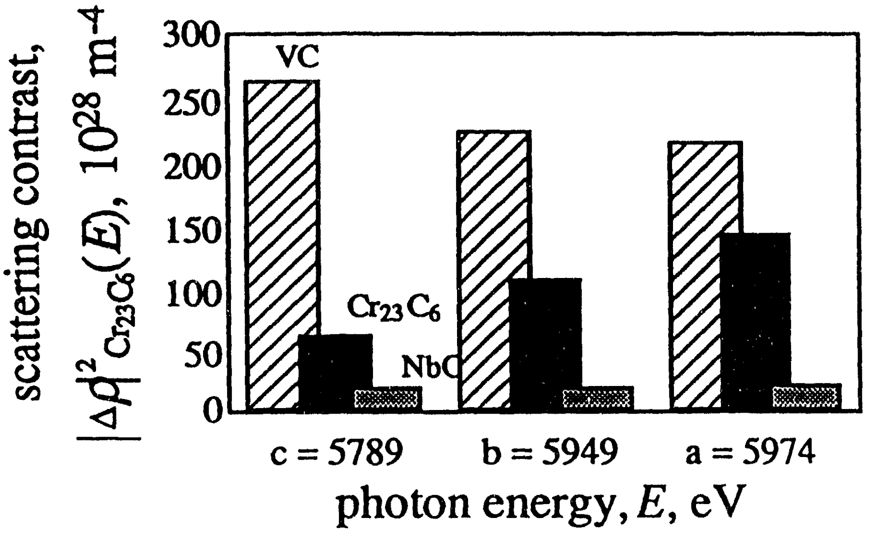

scattering contrast, $|\Delta\rho|^2_{Cr_{23}C_6}(E)$, 10^{28} m^{-4}
300
250
200
150
100
50
0
VC
$Cr_{23}C_6$
NbC
c = 5789
b = 5949
a = 5974
photon energy, E, eV

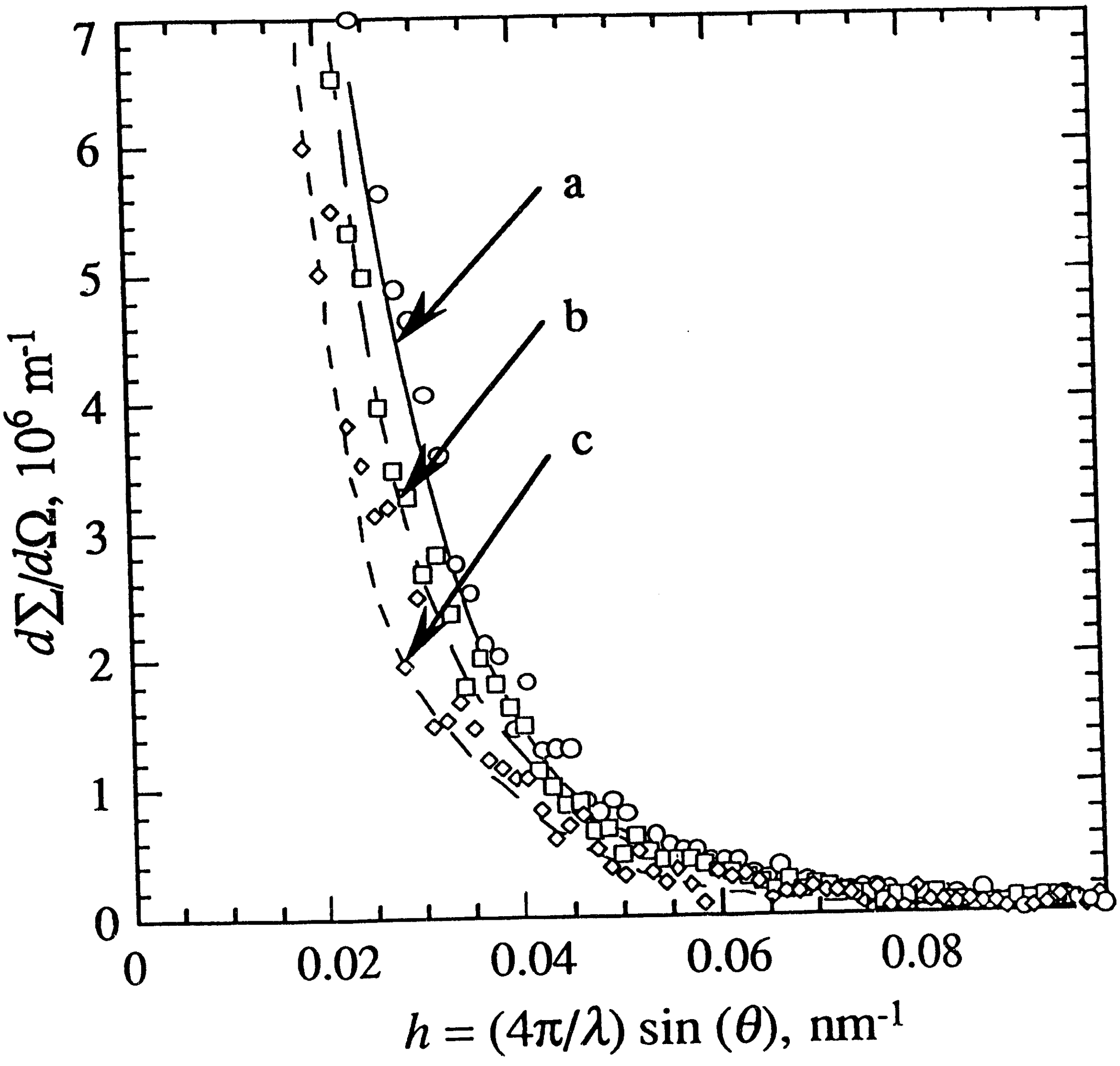
7
6
5
4
3
2
1
0
0
0.02
0.04
0.06
0.08
$d\Sigma/d\Omega$, 10^6 m^{-1}
$h = (4\pi/\lambda)\sin(\theta)$, nm^{-1}
a
b
c

⑤

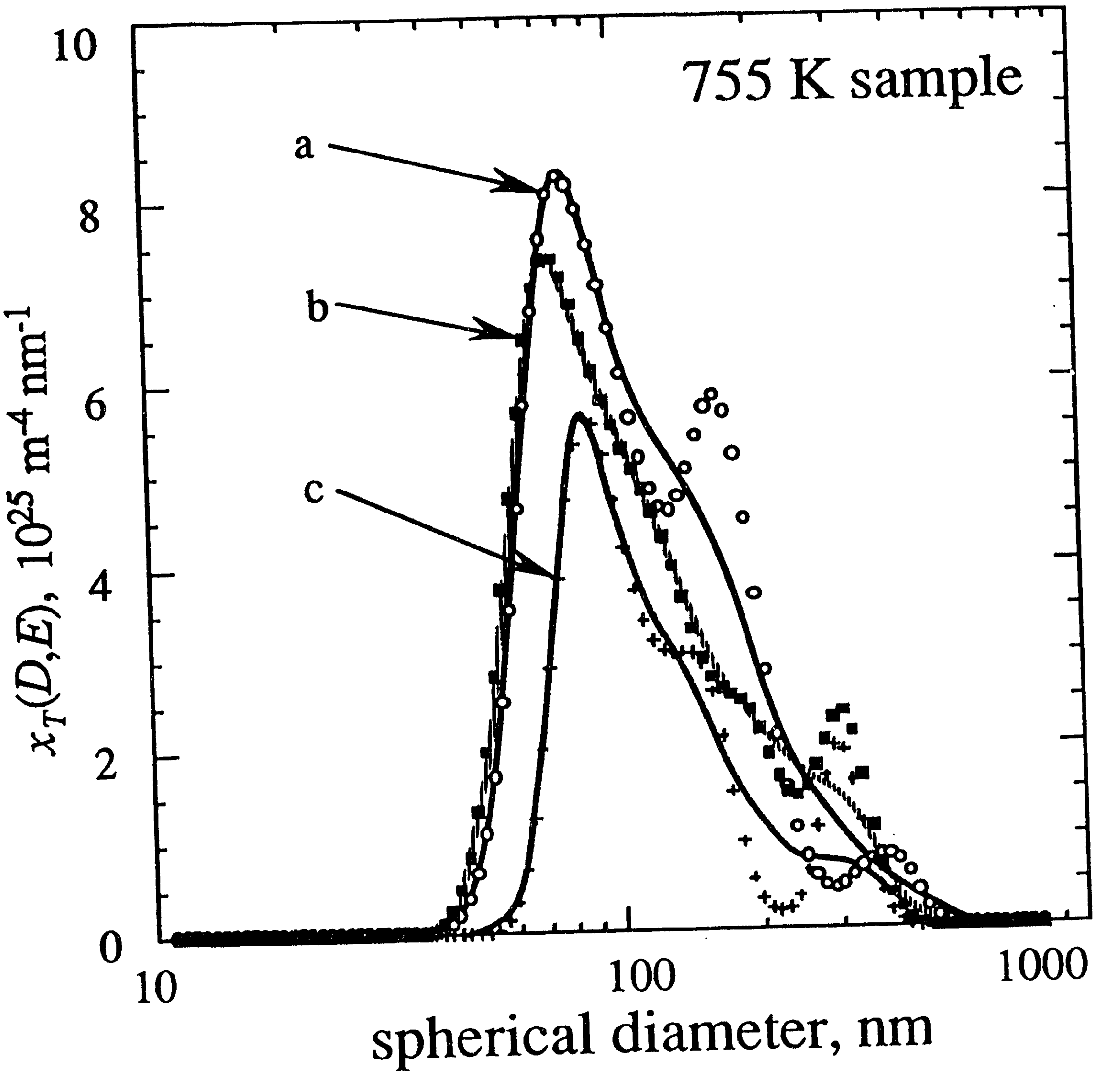
755 K sample
a
b
c
$x_T(D,E)$, 10^{25} m^{-4} nm^{-1}
0
2
4
6
8
10
10
100
1000
spherical diameter, nm

⑥

ASAXS Gradient Method

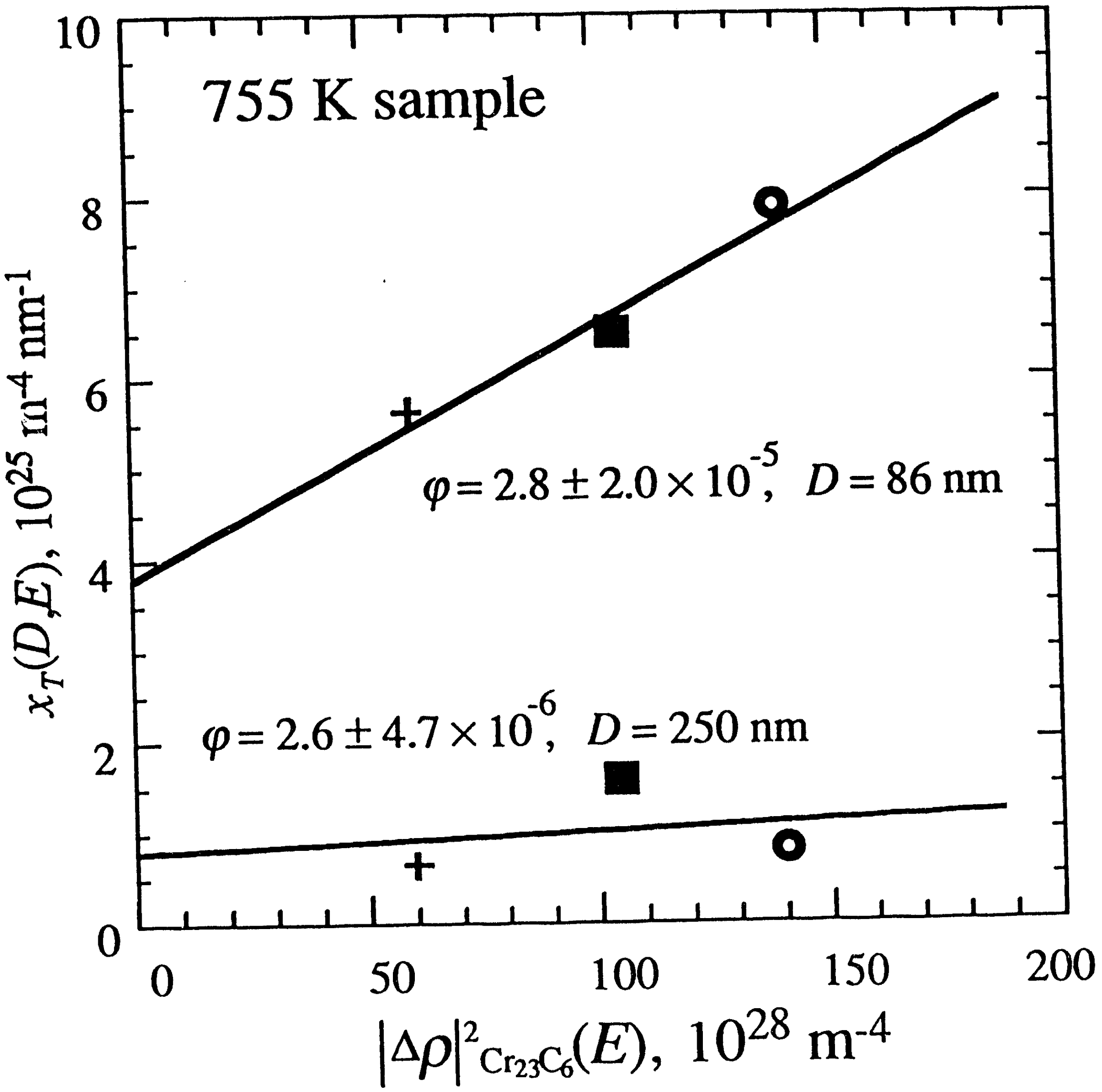

2

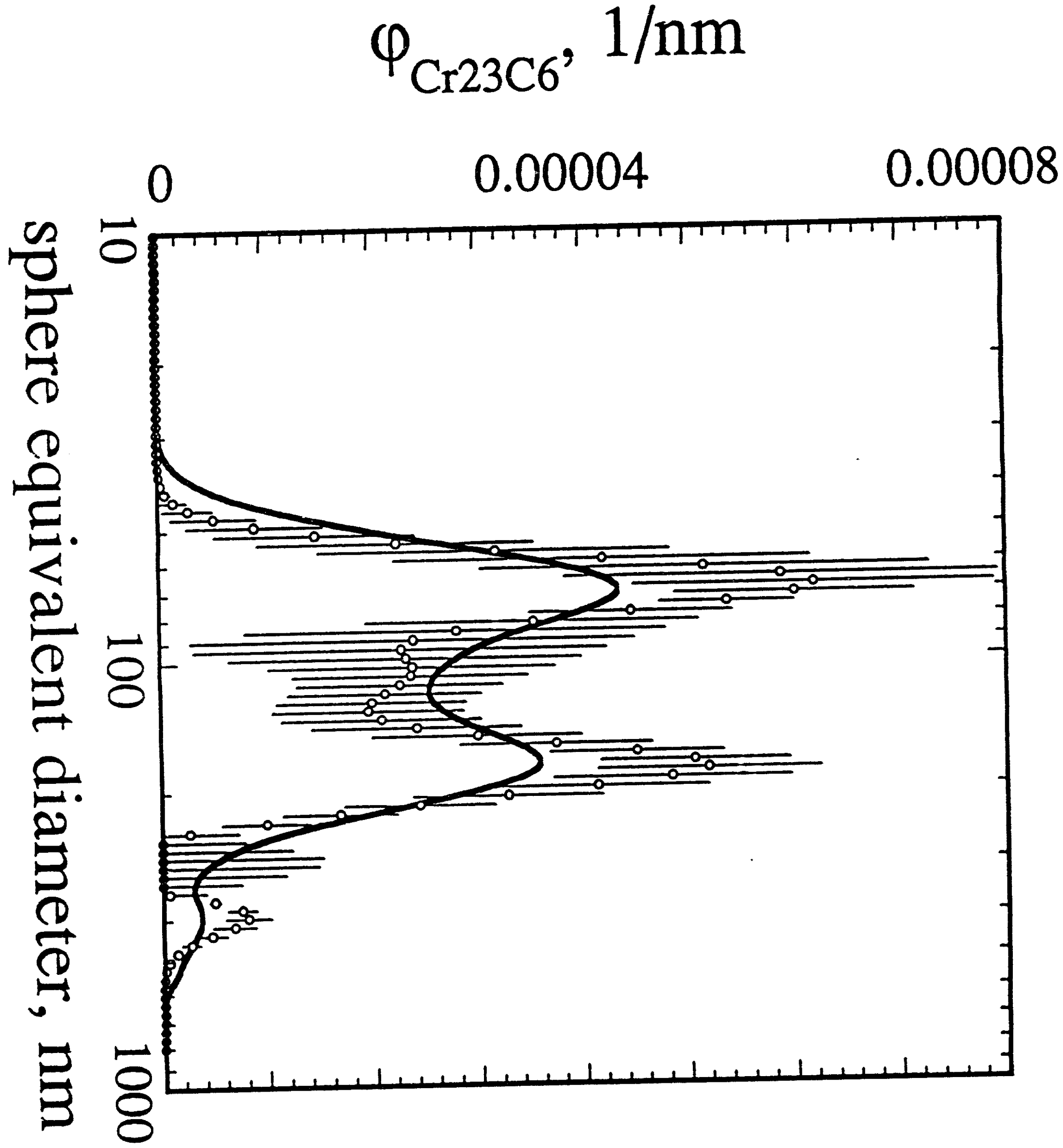

φ_{Cr23C6}, 1/nm
0
0.00004
0.00008
10
100
1000
sphere equivalent diameter, nm

DATE
FILMED
6/15/94

END